Oncogene (2019) 38:5469–5485
https://doi.org/10.1038/s41388-019-0803-9

ARTICLE

# Tumor-associated macrophage-secreted 14-3-3ζ signals via AXL to promote pancreatic cancer chemoresistance

Gabriele D'Errico[1,2] · Marta Alonso-Nocelo[1,3,4] · Mireia Vallespinos[1,3,4] · Patrick C. Hermann[5] · Sonia Alcalá[1,3,4] · Coral Pedrero García[1,3,4] · Laura Martin-Hijano[1,3,4] · Sandra Valle[1,3,4] · Julie Earl[4,6,7] · Chiara Cassiano[8] · Luis Lombardia[9] · Jaime Feliu[2,6] · Maria Chiara Monti[8] · Thomas Seufferlein[5] · Laura García-Bermejo[10] · Paola Martinelli[11] · Alfredo Carrato[4,6,7] · Bruno Sainz Jr.[1,3,4]

Received: 30 September 2018 / Revised: 28 February 2019 / Accepted: 16 March 2019 / Published online: 1 April 2019


## Abstract

Pancreatic ductal adenocarcinoma (PDAC) is an inherently chemoresistant tumor. Chemotherapy leads to apoptosis of cancer cells, and in previous studies we have shown that tumor-associated macrophage (TAM) infiltration increases following chemotherapy in PDAC. Since one of the main functions of macrophages is to eliminate apoptotic cells, we hypothesized that TAMs phagocytose chemotherapy-induced apoptotic cells and secrete factors, which favor PDAC chemoresistance. To test this hypothesis, primary human PDAC cultures were treated with conditioned media (CM) from monocyte-derived macrophage cultures incubated with apoptotic PDAC cells (MØ$^{Apop}$CM). MØ$^{Apop}$CM pretreatment rendered naïve PDAC cells resistant to Gemcitabine- or Abraxane-induced apoptosis. Proteomic analysis of MØ$^{Apop}$CM identified YWHAZ/14-3-3 protein zeta/delta (14-3-3ζ), a major regulator of apoptotic cellular pathways, as a potential mediator of chemoresistance, which was subsequently validated in patient transcriptional datasets, serum samples from PDAC patients and using recombinant 14-3-3ζ and inhibitors thereof. Moreover, in mice bearing orthotopic PDAC tumors, the antitumor potential of Gemcitabine was significantly enhanced by elimination of TAMs using clodronate liposomes or by pharmacological inhibition of the Axl receptor tyrosine kinase, a 14-3-3ζ interacting partner. These data highlight a unique regulatory mechanism by which chemotherapy-induced apoptosis acts as a switch to initiate a protumor/antiapoptotic mechanism in PDAC via 14-3-3ζ/Axl signaling, leading to phosphorylation of Akt and activation of cellular prosurvival mechanisms. The data presented therefore challenge the idea that apoptosis of tumor cells is therapeutically beneficial, at least when immune sensor cells, such as macrophages, are present.

These authors contributed equally: Gabriele D'Errico, Marta Alonso-Nocelo

**Supplementary information** The online version of this article (https://doi.org/10.1038/s41388-019-0803-9) contains supplementary material, which is available to authorized users.

✉ Bruno Sainz
bruno.sainz@uam.es

[1] Department of Biochemistry, Universidad Autónoma de Madrid (UAM), Madrid, Spain

[2] Department of Medical Oncology, La Paz University Hospital, Madrid, Spain

[3] Department of Cancer Biology, Instituto de Investigaciones Biomédicas "Alberto Sols" (IIBM), CSIC-UAM, Madrid, Spain

[4] Chronic Diseases and Cancer Area 3—Instituto Ramón y Cajal de Investigación Sanitaria (IRYCIS), Madrid, Spain

[5] Department of Internal Medicine I, Ulm University, Ulm, Germany

[6] Biomedical Research Network in Cancer (CIBERONC, CB16/12/00446 and CB16/12/00398), Madrid, Spain

[7] Medical Oncology Department, Ramón y Cajal University Hospital, Alcala University, Madrid, Spain

[8] Department of Pharmacy, University of Salerno, Fisciano, Salerno, Italy

[9] Molecular Diagnostics Unit—Clinical Research Programme, Spanish National Cancer Research Centre (CNIO), Madrid, Spain

[10] Biomarkers and Therapeutic Targets Group—IRYCIS, Madrid, Spain

[11] Institute for Cancer Research, Comprehensive Cancer Center, Medical University Wien, Vienna, Austria

## Introduction

Pancreatic ductal adenocarcinoma (PDAC), the most frequent form of pancreatic cancer, is considered the deadliest

of all solid cancers. While currently the fourth most frequent cause of cancer-related deaths worldwide, by 2030, PDAC is expected to become the second-leading cause of cancer-related deaths, trailing only lung cancer [1]. At the clinical level, PDAC is characterized by late diagnosis due to a lack of early and specific symptoms, and as such, approximately 80% of patients present with nonresectable disseminated/advanced disease [2]. For these patients, treatment options include combinations of 5-FU, Oxaliplatin and Irinotecan or Gemcitabine and Abraxane; however, therapeutic intervention only slightly improves overall survival beyond 6 months and very rarely result in long-term (>5 years) progression-free survival [3].

Over the past decade we have come to appreciate that cancer cells need the tumor microenvironment to maintain tumor growth, metastasize and proliferate in the presence of therapeutic challenges. Tumor-associated macrophages (TAMs), a main component of the tumor mass in many malignant carcinomas including PDAC [4], can represent up to 50% of the tumor stroma and are believed to be pivotal at all levels of tumorigenesis due to protumorigenic factors secreted by these cells [5]. For example, Nielsen et al. showed that macrophage-secreted granulin, a secreted glycoprotein that stimulates fibroblast migration, facilitates successful PDAC cell metastasis in the liver by activating resident hepatic stellate cells into myofibroblasts, which in turn promotes liver fibrosis via secretion of periostin [6]. Thus, at the functional level, TAMs can modulate the primary and secondary microenvironments to facilitate tumor cell dissemination or secondary metastatic lesion growth.

TAM-secreted growth factors, chemokines, and cytokines (IL-17, IL-6, IL-8, TNFα, TGF-β1) can also orchestrate numerous events critical for tumor progression and metastasis (reviewed in [7]). Specific to PDAC, we have shown that the cationic antimicrobial peptide 18/leucine leucine-37 (LL-37) and free interferon-stimulated gene 15 (ISG15) are secreted by TAMs and can activate pancreatic cancer stem cells, promoting tumor growth, epithelial to mesenchymal transition (EMT) and metastasis [8, 9]. Recent evidence now also implicates TAMs as critical players in tumor cell chemoresistance [10–13]; however, more studies in this area are still needed to determine the molecular mechanisms by which TAMs may promote tumor chemoresistance, specifically in PDAC.

Chemotherapy can lead to cancer cell necrosis or apoptosis. Numerous studies have shown that post-treatment tumor cell death can be perceived by the immune system as a repair signal, initiating a wound-healing response that can favor sustained tumor growth and even tumor chemoresistance via immune cell-secreted factors (reviewed in [14]). We hypothesized that TAMs sense apoptotic cancer cells and put into motion a process to reduce further apoptosis by releasing factor(s) that inhibit apoptosis (i.e. promoting chemoresistance). In line with this hypothesis, we show that macrophages secrete the antiapoptotic factor YWHAZ/14-3-3 zeta/delta (14-3-3ζ) following phagocytosis of apoptotic PDAC cells, rendering naïve PDAC cells resistant to chemotherapeutic-induced apoptosis. In addition, we show in an in vivo orthotopic transplantation model that macrophage elimination or targeting 14-3-3ζ signaling using the Axl receptor tyrosine kinase inhibitor SGI-7079 [15] can improve chemotherapeutic efficacy, resulting in reduced tumor growth in mice. As such, we propose that neutralizing 14-3-3ζ or targeting the 14-3-3ζ/Axl axis may represent a mechanism to overcome TAM-mediated chemoresistance in PDAC.

## Results

### PDAC cell apoptosis promotes macrophage polarization

TAM infiltration is a hallmark of PDAC, and the increased expression of TAM markers, such as CD163 or MSR1, correlate with reduced overall survival [16] (Supplementary Fig. S1A and B). To evaluate TAM infiltration during chemotherapy, we analyzed macrophage infiltration and apoptosis in PDAC tumors from patients treated with Gemcitabine, Gemcitabine and radiotherapy or Gemcitabine and Abraxane and in untreated PDAC samples for comparison. Immunohistochemical (IHC) analysis consistently showed CD163-positive cell infiltrates across samples. Likewise, TdT-mediated dUTP nick-end labeling (TUNEL) analysis showed TUNEL-positive apoptotic cells in Formalin-Fixed Paraffin-Embedded (FFPE) sections of therapy-treated samples compared with scarce staining in samples from untreated control patients (Fig. 1a and Supplementary Fig. S2A). Since one of the main functions of macrophages is to eliminate apoptotic cells [17], we hypothesized that apoptotic PDAC cells may promote macrophage polarization towards a more TAM-like phenotype following their phagocytosis. To test this hypothesis, we first confirmed that CD163-positive macrophages colocalize with TUNEL-positive cells in serial sections of the aforementioned samples (Fig. 1b and Supplementary Fig. S2B). Next, we determined an appropriate dose of Gemcitabine or Abraxane that could induce a greater than twofold increase in apoptosis (Supplementary Fig. S3) in the primary PDX-derived human PDAC cultures Panc354 (*TP53* mutant) and Panc286 (*TP53* wild-type (wt)) (Supplementary Fig. S4). Using 1 µg/ml of Gemcitabine, green-labeled apoptotic Panc354 cells (with PKH67) were cocultured with red-labeled nonpolarized monocyte-derived macrophages (with DilC) to measure colocalization, and follow-up analyses showed that macrophages efficiently phagocytosed

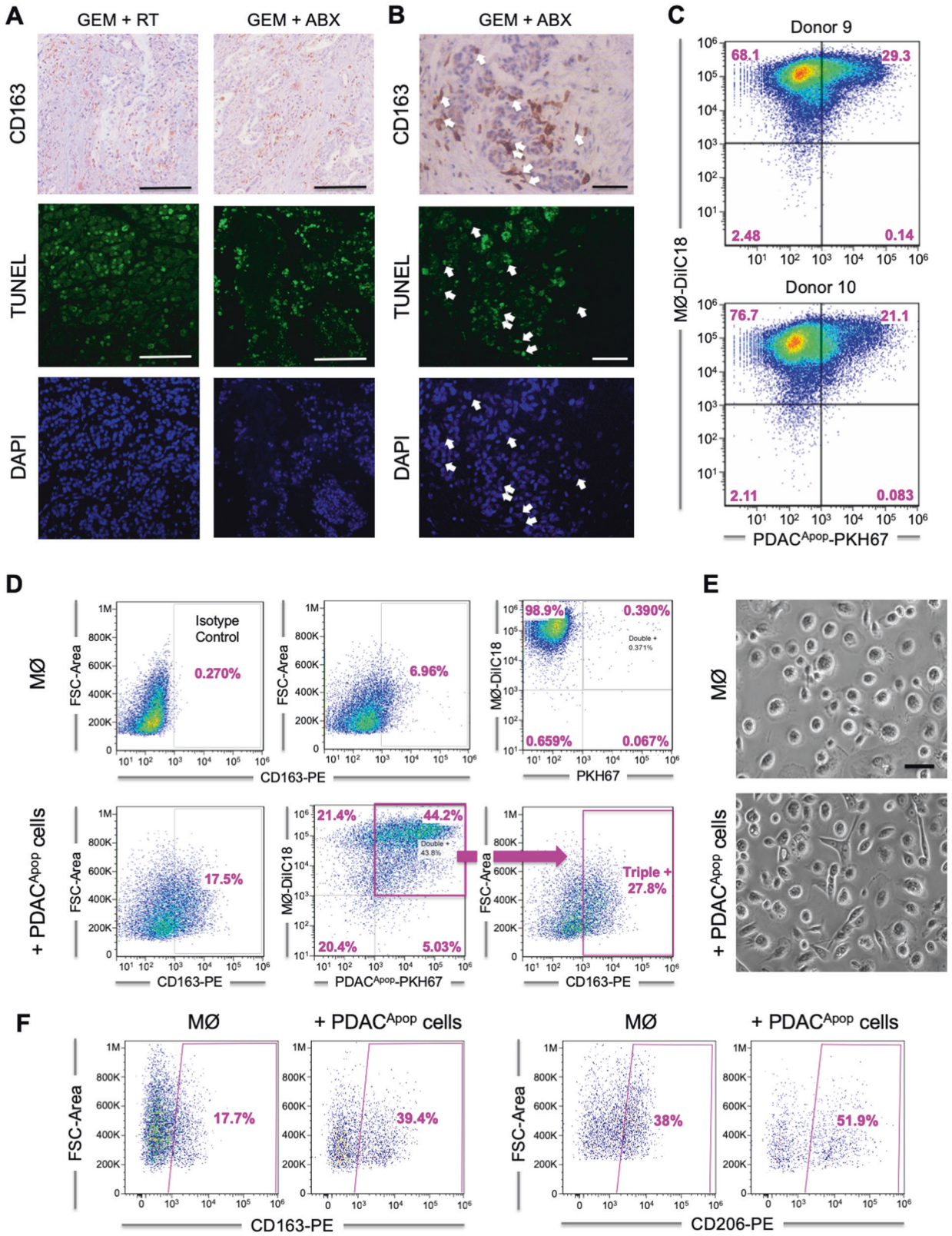


apoptotic Panc354 cells (Fig. 1c and Supplementary Fig. S5A and B). We additionally assessed the CD163-positive (i.e. "M2"-like) population within the double-positive (DilC18$^+$/PKH67$^+$) population 12 h following coincubation of DilC18-stained macrophages with PKH67-stained apoptotic cells, and we observed that 20−25% of the

◀ **Fig. 1** PDAC cell apoptosis and macrophage conditioning. **a** CD163 (TAM marker), terminal deoxynucleotide transferase dUTP nick-end labeling (TUNEL) and DAPI expression in FFPE PDAC samples from patients treated with Gemcitabine (GEM) plus radiotherapy (RT) or GEM plus Abraxane (ABX). Scale bar: 50 µm. **b** CD163, TUNEL and 4′,6-diamidino-2-phenylindole (DAPI) expression in FFPE serial sections from GEM plus ABX-treated patients. Arrows indicate colocalization. Scale bar: 50 µm. **c** Flow cytometric analysis of macrophage (MØ) cultures from $n = 2$ different donors incubated for 4 h with apoptotic PDAC ($PDAC^{Apop}$) cells. $PDAC^{Apop}$ cells were labeled with PKH67 and MØ were labeled with DilC 8 h post coincubation. **d** Flow cytometric analysis of macrophage (MØ) cultures ($n = 1$) incubated for 4 h with apoptotic PDAC ($PDAC^{Apop}$) cells. $PDAC^{Apop}$ cells were labeled with PKH67 and MØ were labeled with DilC and additionally stained for CD163 8 h post coincubation. **e** Light micrographs of MØ and MØ incubated with $PDAC^{Apop}$ cells for 4 h ($n = 1$). **f** Flow cytometric analysis of CD163 and CD206 cell surface expression for MØs shown in panel (**e**). All cytometry gates were established based on isotype controls. PDAC Pancreatic ductal adenocarcinoma, TAM tumor-associated macrophage

macrophages were CD163-positive (Fig. 1d), indicating that the major subpopulation of macrophages that participates in the phagocytosis process are non-M2 macrophages, as would be expected since M1 macrophages have higher phagocytic capacity. Interestingly, however, macrophages cocultured with apoptotic PDAC cells for 48 h showed a more elongated morphology (Fig. 1e) and increased the expression of the M2 macrophage cell surface markers CD163 and CD206 (Fig. 1f), suggesting polarization to an alternatively activated "M2"-like state over time, which was partially observed as early as 12 h (Fig. 1d). Polarization was also confirmed by assessing the expression of TAM-PDAC-associated transcripts, specifically *ACTA1*, *COL1A1*, *COL3A1*, *CTGF*, *LOX*, *LOXL2*, *MMP3* and *SPARC* (Supplementary Fig. S5C). All TAM-PDAC mRNAs, except *SPARC*, significantly increased in macrophages following phagocytosis of apoptotic PDAC cells.

## Macrophages that phagocytose apoptotic PDAC cells secrete factors that promote PDAC chemoresistance and self-renewal

To determine if the aforementioned TAM-like macrophages secrete factors that could promote PDAC cell chemoresistance, an in vitro system to produce conditioned media (CM) from monocyte-derived macrophage cultures (MØ) cocultured with apoptotic PDAC cells was established (Fig. 2a). Panc354 cells pretreated with CM from MØs of different donors cocultured with apoptotic PDAC cells ($MØ^{Apop}CM$) were highly resistant to subsequent Gemcitabine treatment (Fig. 2b). Specifically, Gemcitabine-mediated apoptosis (early and late) was reduced in cultures pretreated with $MØ^{Apop}CM$ by greater than twofold and cell viability increased to almost basal untreated levels. To confirm this observation, the chemoresistance of Panc354 (*TP53* mutant), Panc185 (*TP53* mutant) and Panc286 (*TP53* wt) cells to Gemcitabine or Abraxane was assessed using control MØCM and $MØ^{Apop}CM$ generated from monocytes isolated from five healthy donors. Shown in Fig. 2c are the combined results of all experiments performed with all donors. While donor-to-donor variability was observed (Fig. 2b), pretreatment of naïve PDAC cultures with $MØ^{Apop}CM$ consistently resulted in significantly reduced chemotherapy-mediated apoptosis (Fig. 2c). Interestingly, while $MØ^{Apop}CM$ was considerably more effective than MØCM at promoting chemoresistance to both Gemcitabine and Abraxane in the *TP53* mutant PDX-derived cell lines (Panc354 and Panc185), in *TP53* wt Panc286 cells, a significant difference in chemoresistance between MØCM and $MØ^{Apop}CM$ was only observed with Abraxane (Fig. 2c).

## Elimination of macrophages enhances PDAC tumor sensitivity to Gemcitabine in vivo

While Gemcitabine induces PDAC cell apoptosis in vivo and in vitro (Fig. 1a and Supplementary Fig. S3), it is well documented that Gemcitabine is ineffective at the level of tumor eradication [18]. Building upon our initial hypothesis, we evaluated whether the anticancer properties of Gemcitabine could be augmented by eliminating macrophages using clodronate-encapsulated liposomes in a syngeneic orthotopic mouse model of PDAC tumorigenesis (Fig. 3a). Neither clodronate treatment nor Gemcitabine treatment alone significantly reduced tumor growth; however, a significant reduction in tumor volume was noted when treatments were combined (Fig. 3b, c). At the histological level, a clear regression in tumor mass as well as tumor cell and stroma content were noted only in mice receiving both clodronate and Gemcitabine (Fig. 3d and Supplementary Fig. S6), with one mouse experiencing complete tumor elimination (right, Fig. 3d). Comparing the other three groups, there was no histological difference in tumor cell differentiation or stroma composition (Supplementary Fig. S6). Regarding the mechanism, clodronate-encapsulated liposomes reduced the percentage of macrophages in vivo (Fig. 3e and Supplementary Fig. S7A and B), and Gemcitabine-induced apoptosis (Fig. 3f and Supplementary Fig. S7C) as expected, indicating that each treatment was effective and thus the observed enhanced effect of Gemcitabine, when used in combination with clodronate-encapsulated liposomes, was likely a result of clodronate-mediated macrophage elimination.

## 14-3-3ζ is expressed in conditioned media and in human PDAC samples

Proteomic and mass spec (MS) analysis of the secretome from macrophages cocultured with apoptotic tumor cells

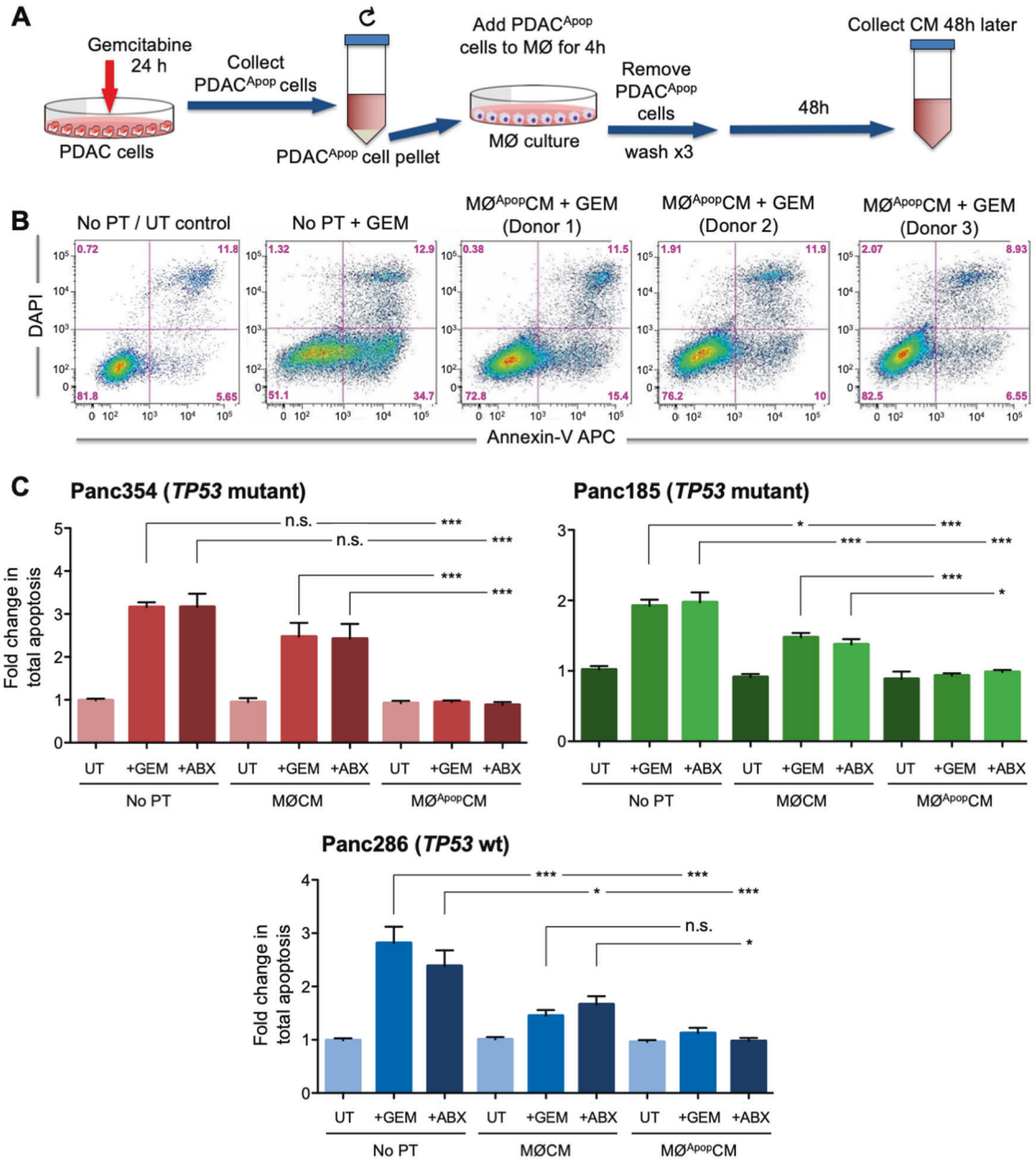


**Fig. 2** PDAC apoptotic cells induce macrophages to secrete factors that promote chemoresistance. **a** Diagram of in vitro system to produce conditioned media (CM) from MØ cultures incubated with PDAC$^{Apop}$ cells. **b** Representative flow cytometric analysis of Annexin-V staining in Panc354 cells 48 h post treatment with GEM. Cell were either non-pretreated (No PT) or pretreated with MØCM or MØ$^{Apop}$CM for 24 h prior to challenge with or without (UT) 1 µg/ml of GEM ($n = 3$). Gating strategies are shown. **c** Fold change in total apoptosis in Panc354, Panc286 or Panc185 cells. Cell were either No PT or pretreated with MØCM or MØ$^{Apop}$CM derived from donors for 24 h prior to chemotherapeutic challenge with or without (UT) GEM (1 µg/ml) or ABX (10 µM), as indicated. Early and late apoptosis was determined 48 h post treatment. Average fold changes were compiled from five separate experiments performed with CM from macrophages of ($n = 5$) different donors. Fold changes were calculated as a function of UT control (set at 1.0). Statistical significance: $*p < 0.05$, $***p < 0.001$. PDAC pancreatic ductal adenocarcinoma

(MØ$^{Apop}$CM) was performed to identify secreted factors that could favor PDAC cell chemoresistance. MS analysis revealed the presence of approximately 23 proteins, considering reliable those proteins identified with a Mascot Score >60 and removing all proteins identified in culture medium (Supplementary Table S1). Since several of these 23 proteins were still identifiable in MØCM and in the live tumor cell secretome, as well as in the secretome from macrophages cocultured with live tumor cells (MØ$^{Live}$CM), we focused on proteins unique to the secretome from macrophages cocultured with apoptotic tumor cells (MØ$^{Apop}$CM) and with a Mascot Score >40 (Fig. 4a and

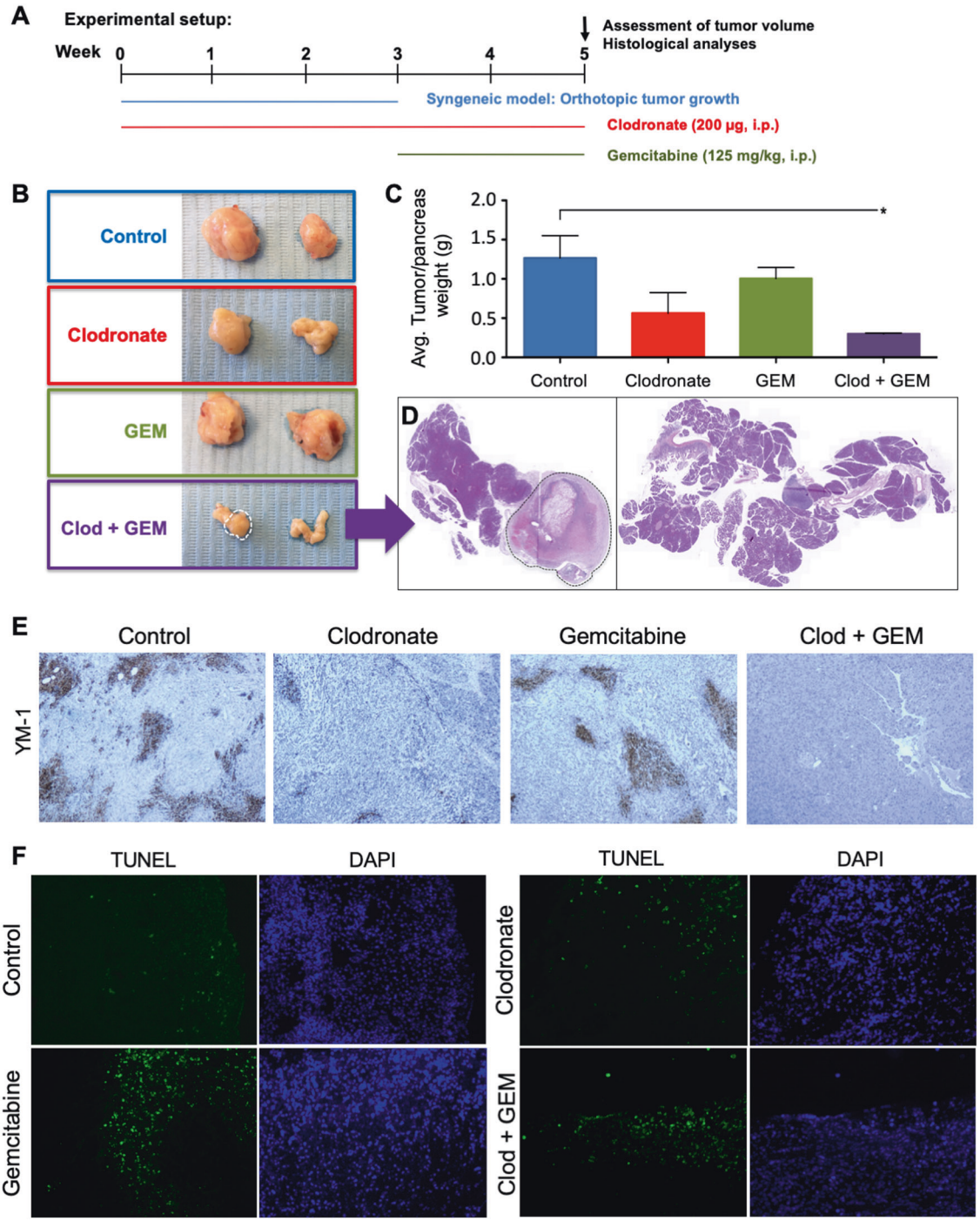


**Fig. 3** Tumor-associated macrophages favor PDAC tumorigenicity and chemoresistance. **a** Experimental set-up for Clodronate (Clod) and Gemcitabine (GEM) in vivo efficacy studies in a syngeneic orthotopic tumor implantation model (i.p. intraperitoneal). **b** Representative images (dashed line marks tumor area), **c** average weight of pancreata and **d** H&E histological images from indicated group. Average (Avg.) tumor weights in panel (**c**) were compiled from two separate experiments each with ($n = 6$) mice per treatment group. Statistical significance: $*p < 0.05$. **e** IHC analysis of YM-1 (murine M2 macrophage marker) staining and **f** TUNEL and DAPI expression in FFPE samples of pancreata from indicated treatment groups. PDAC pancreatic ductal adenocarcinoma, IHC Immunohistochemistry, TUNEL TdT-mediated dUTP nick-end labeling

Supplementary Table S2). Of the resulting 17 proteins, three proteins were identified with putative antiapoptotic functions, including YWHAZ/14-3-3ζ, TIMP metallopeptidase inhibitor 1 (TIMP1) and Hornerin (HORN). 14-3-3ζ showed a high Mascot score [120], indicating that its identification was not a random event, and a high number of

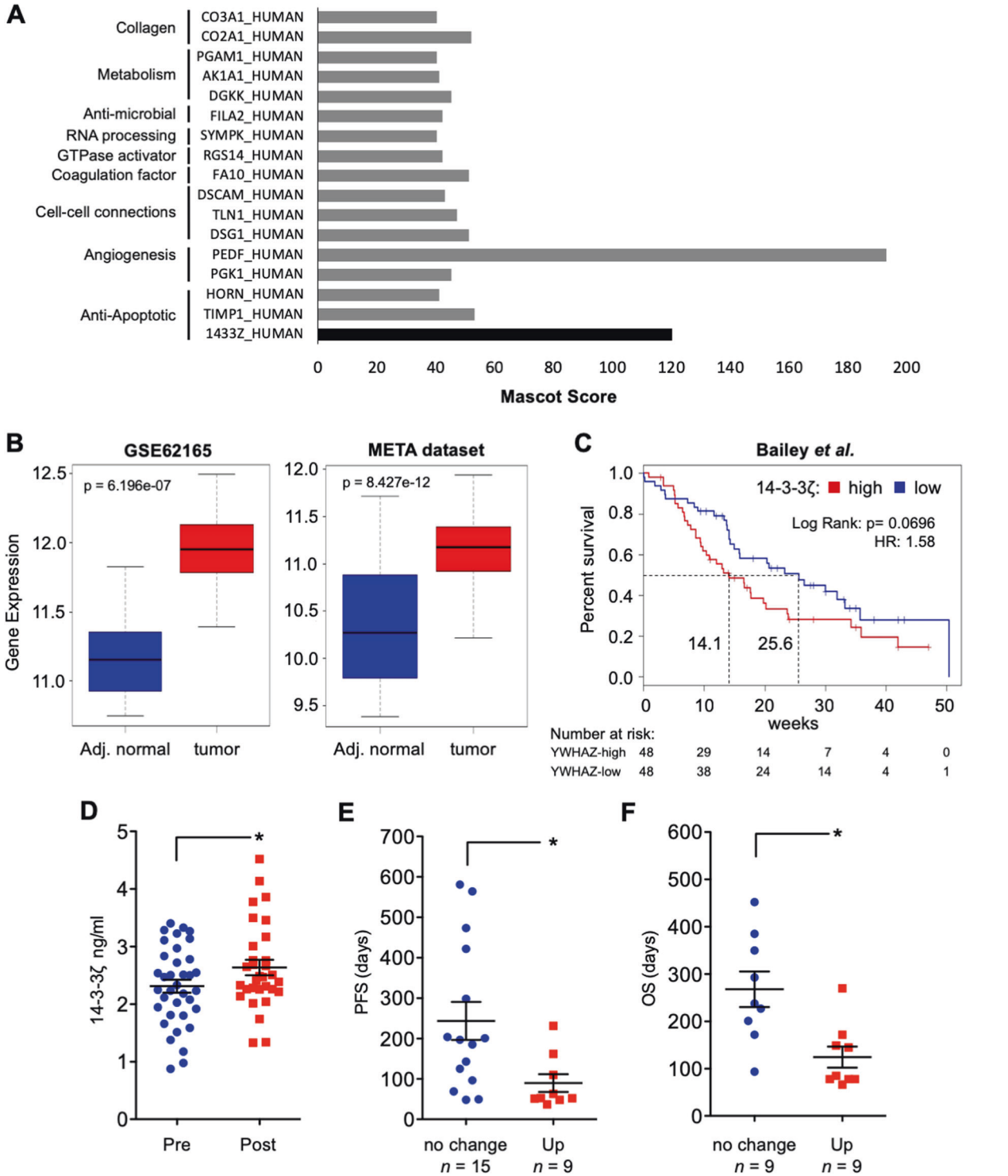


**Fig. 4** 14-3-3ζ is expressed in MØ$^{Apop}$CM and in human PDAC samples. **a** Proteomics analysis of proteins enriched in the secretome of macrophages cocultured with apoptotic tumor cells (MØ$^{Apop}$CM). Shown are the Mascot scores for each identified protein (*x*-axis) and putative functions (*y*-axis). **b** Boxplots showing the differential expression of 14-3-3ζ in PDAC samples vs. normal adjacent tissue in two independent series of transcriptomics data (left: $n = 13$ adj. normal, $n = 118$ tumor; right: $n = 70$ adj. normal, $n = 108$ tumor). **c** Kaplan−Meier curve showing the overall survival of PDAC patients, stratified according to the median value of 14-3-3ζ expression ($n = 96$). The hazard ratio (HR) and number of patients at risk are shown. **d** Quantification of 14-3-3ζ levels in the serum of 35 matched PDAC patients pre- and post chemotherapy. Scatter plots showing **e** progression-free survival (PFS) or **f** overall survival (OS) of patients with no significant change or with a greater than 15% increase (Up) in 14-3-3ζ levels. Statistical significance: $^*p < 0.05$. PDAC pancreatic ductal adenocarcinoma

matches [28] representing the number of MS/MS spectra matched to this protein. Since 14-3-3ζ is a secreted protein capable of direct diffusion through cell membranes [19] and a member of a larger family of highly conserved dimeric proteins that have been shown to mediate antiapoptotic signaling [20], it was designated as the top candidate for follow-up.

While 14-3-3ζ overexpression has been observed in different tumor entities [21, 22], its expression and role in PDAC has not been rigorously examined. Using three publicly available transcriptome datasets (META dataset [23], Janky et al. [24] and Jandaghi et al. [25]], the transcriptional levels of 14-3-3ζ expression were evaluated and, as expected, 14-3-3ζ expression was significantly elevated in whole pancreatic tumor samples vs. adjacent normal tissue (Fig. 4b and Supplementary Fig. S8A). Interestingly, however, in the 68 pancreatitis samples from the Jandaghi et al. dataset, 14-3-3ζ expression was unchanged (Fig. S8A), indicating that its expression may either be tumor specific or a consequence of chemotherapy as most samples included in many datasets are from surgical samples from patients that have received chemotherapy. For the Bailey et al. series [26], well-annotated clinical data were available, and although not significant ($p = 0.0696$), a clear deviation and decrease in median overall survival of 14-3-3ζ high-expressing patients compared to the 14-3-3ζ low-expressing patients was appreciated (Fig. 4c). To gain insight into the function of 14-3-3ζ in PDAC, GSEA comparing the samples belonging to the top and bottom quartiles of 14-3-3ζ expression was performed. Using the "Hallmark" genesets collection, we observed significantly and commonly enriched pathways across all series, including p53 and mTOR signaling, apoptosis and G2M checkpoint (Supplementary Fig. S9).

Finally, ELISA analysis of 14-3-3ζ protein levels in serum samples obtained before and following chemotherapy from 34 PDAC patients (Supplementary Table S3) revealed a significant increase in 14-3-3ζ levels following chemotherapy (Fig. 4d). To evaluate the changes on a patient-to-patient level, we calculated the fold increase in 14-3-3ζ after treatment. For those patients where progression-free survival (PFS) or overall survival (OS) data were available, we observed a significant decrease in survival when 14-3-3ζ levels significantly increased following chemotherapy (Fig. 4e, f) compared to patients showing a decrease or no change. Of note, no correlations could be made with respect to the type of chemotherapy used, age, sex or staging.

## 14-3-3ζ promotes PDAC chemoresistance

Having observed clear and consistent results with Panc354, we used this cell line to further study 14-3-3ζ at the molecular level in vitro. In concordance with the dataset series (Fig. 4b), 14-3-3ζ mRNA was expressed at high levels in PDAC cells and increased when apoptosis was induced (Fig. 5a). In macrophages, 14-3-3ζ mRNA levels increased by twofold when incubated with apoptotic PDAC cells; however, at the protein level no apparent increase in intracellular 14-3-3ζ was observed (lane 2 vs. 1, Fig. 5a, b). We reconciled this difference by the fact that significant amounts of 14-3-3ζ were detected in the secretome of macrophages incubated with apoptotic PDAC cells (lane 6 vs. 5, Fig. 5b), which additionally validates the proteomic MS data obtained. Finally, a notable increase in 14-3-3ζ was observed in Panc354 cells treated with MØ$^{Apop}$CM (lane 4 vs. 3, Fig. 5b). Importantly, we show that 14-3-3ζ detected in MØ$^{Apop}$CM was due to phagocytosis of PDAC$^{Apop}$cells by inhibiting phagocytosis with 10 µM colchicine plus 2 µM cytochalasin D (Fig. 5c), as previously described [27], and performing WB analysis on CM harvested from macrophages in the presence or absence of the inhibitors (Fig. 5d).

To test whether 14-3-3ζ alone can mediate chemoresistance, PDAC cells were pretreated with recombinant 14-3-3ζ (r14-3-3ζ) and apoptosis was determined post chemotherapeutic challenge. Cells pretreated with r14-3-3ζ showed enhanced chemoresistance in multiple experiments (Fig. 5e, f), and more importantly, this protective effect could be abrogated by blocking r14-3-3ζ with an anti-14-3-3ζ polyclonal antibody (Fig. 5f), demonstrating specificity and at the same time suggesting that 14-3-3ζ neutralization may be therapeutically beneficial.

## 14-3-3ζ drives chemoresistance by activating AXL-mediated prosurvival pathways

While more than 100 14-3-3ζ binding partners have been identified to date [28], Reichl et al. recently showed that the receptor tyrosine kinase Axl binds to 14-3-3ζ, this interaction is necessary for Axl-mediated downstream events [29], and Axl has been implicated in PDAC chemoresistance [30]. As such, *AXL* expression levels were evaluated in normal adjacent tissue, PDAC samples and pancreatitis tissues in the Jandaghi et al. series (Supplementary Fig. S8B). Likewise, *AXL* levels were quantified in PDAC cells treated with MØ$^{Apop}$CM or r14-3-3ζ, and in both cases, relative mRNA levels of Axl increased (Fig. 6a). In addition, and more importantly, the phosphorylation of Axl and AKT, the latter being an essential downstream mediator of phospho-Axl [31] and known binding partner of 14-3-3ζ [32], were induced in Panc354 cells treated with r14-3-3ζ (Fig. 6b), highlighting that 14-3-3ζ can activate important prosurvival proteins, via phosphorylation of the receptor tyrosine kinase Axl. To confirm the latter, we used the Axl-specific inhibitor SGI-7079 [15] and no longer observed phosphorylation of both Axl and AKT in the presence of r14-3-3ζ (Fig. 6b). More importantly, SGI-7079 also reversed the capacity of r14-3-3ζ to protect Panc354 cells from Gemcitabine-induced apoptosis (Fig. 6c–e).

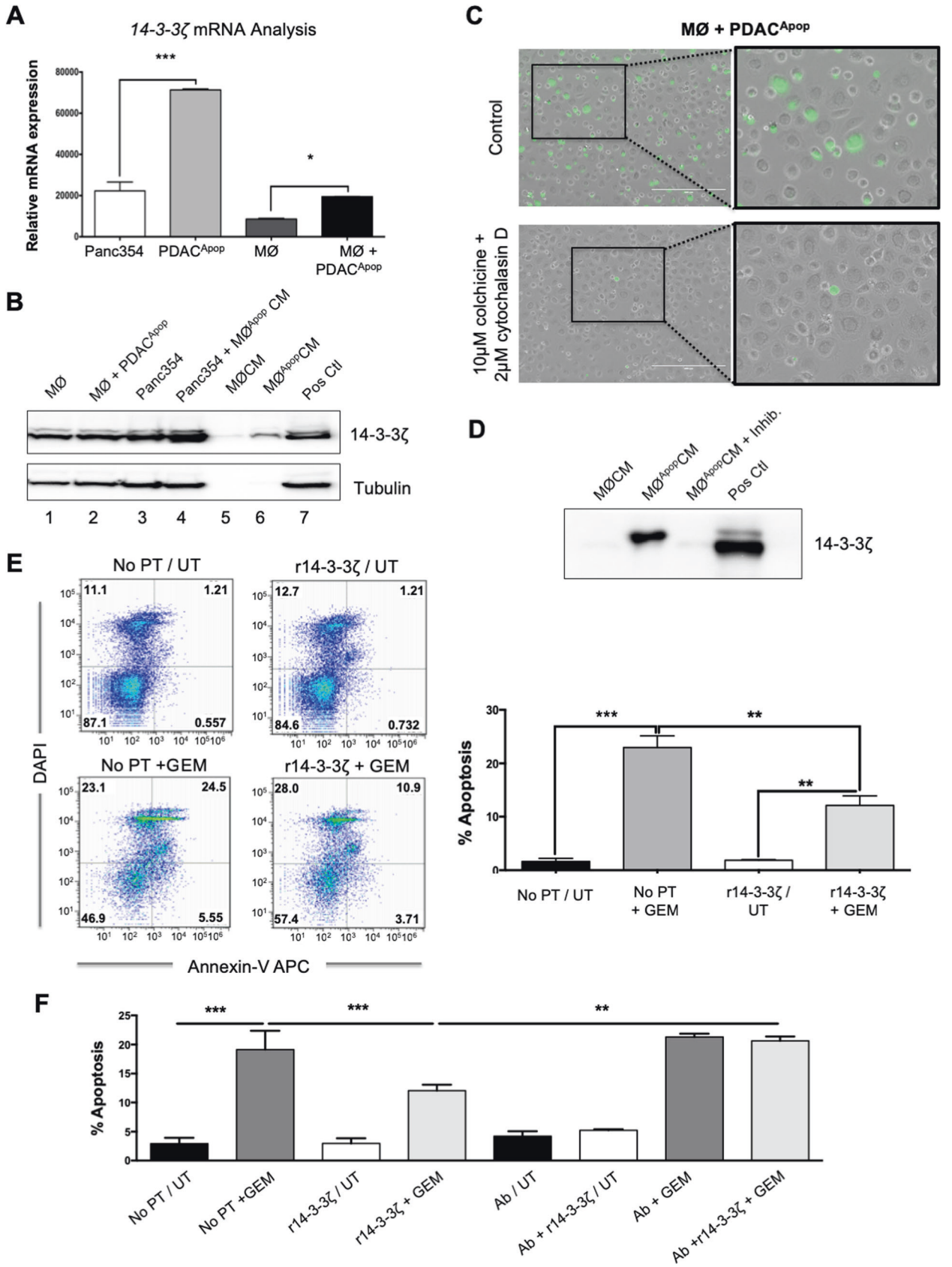
A
14-3-3ζ mRNA Analysis
Relative mRNA expression
Panc354
PDAC^Apop
MØ
MØ + PDAC^Apop
B
MØ
MØ + PDAC^Apop
Panc354
Panc354 + MØ^Apop CM
MØCM
MØ^ApopCM
Pos Ctl
14-3-3ζ
Tubulin
C
MØ + PDAC^Apop
Control
10μM colchicine + 2μM cytochalasin D
D
MØCM
MØ^ApopCM
MØ^ApopCM + Inhib.
Pos Ctl
14-3-3ζ
E
No PT / UT
r14-3-3ζ / UT
No PT +GEM
r14-3-3ζ + GEM
DAPI
Annexin-V APC
% Apoptosis
No PT / UT
No PT + GEM
r14-3-3ζ / UT
r14-3-3ζ + GEM
F
% Apoptosis
No PT / UT
No PT +GEM
r14-3-3ζ / UT
r14-3-3ζ + GEM
Ab / UT
Ab + r14-3-3ζ / UT
Ab + GEM
Ab +r14-3-3ζ + GEM

◀ **Fig. 5** 14-3-3ζ promotes PDAC chemoresistance. **a** RTqPCR analysis of 14-3-3ζ relative mRNA expression levels in Panc354 cells, apoptotic Panc354 cells ($PDAC^{Apop}$), naive MØ or MØ incubated for 4 h with $PDAC^{Apop}$. mRNA expression levels for each target gene are normalized to ß-actin levels ($n = 4$ samples per group). **b** Expression of 14-3-3ζ, detected by western blotting, in total lysates from naive MØ, MØ incubated for 4 h with $PDAC^{Apop}$, Panc354 cells, or Panc354 cells treated for 24 h with $MØ^{Apop}$CM, or in concentrated CM from naïve MØ (MØCM) or MØ incubated for 4 h with $PDAC^{Apop}$ ($MØ^{Apop}$CM). Tubulin was used as a loading control. Total Raji cell lysate was used as a positive control (Pos Ctl). Blot representative of two independent experiments. **c** Representative light and immunofluorescence overlaid micrographs of MØ cultures incubated for 4 h with PKH67-stained $PDAC^{Apop}$ cells in the presence or absence of the phagocytosis inhibitors (10 µM colchicine + 2 µM cytochalasin D). **d** Expression of 14-3-3ζ, detected by western blotting, in concentrated CM from naïve MØ (MØCM) or MØ incubated for 4 h with $PDAC^{Apop}$ ($MØ^{Apop}$CM) with or without phagocytosis inhibitors (Inhib). Tubulin was used as a loading control. Total Raji cell lysate was used as a positive control (Pos Ctl). **e** Representative flow cytometric analysis of Annexin-V staining in Panc354 cells 48 h post treatment with GEM. Cells were either non-pretreated (No PT) or pretreated with r14-3-3ζ for 6 h prior to challenge with or without (UT) 1 µg/ml of GEM. Gating strategies are shown (left). Quantification of total apoptosis (right). Average of two independent experiments. **f** Quantification of total apoptosis in Panc354 cells 48 h post treatment with GEM. Cells were either non-pretreated (No PT) or pretreated for 6 h with r14-3-3ζ alone, an anti-14-3-3ζ antibody (1 µg/ml) or a combination of both prior to challenge with or without (UT) 1 µg/ml of GEM. Average of two independent experiments ($n = 3$ samples/experiment). Statistical significance: $^{*}p < 0.05$, $^{**}p < 0.01$, $^{***}p < 0.001$. PDAC pancreatic ductal adenocarcinoma

## Inhibition of Axl potentiates the anticancer efficacy of Gemcitabine in vivo

Axl signaling potentiates prosurvival, proproliferation and prometastasis pathways in cancer [33], and in PDAC, Axl signaling has been shown to play an important role in cellular plasticity, metastasis and chemoresistance [30, 34]. Based on our findings linking 14-3-3ζ and Axl signaling in PDAC chemoresistance, SGI-7079 was used to block Axl signaling in the syngeneic mouse model of PDAC tumorigenesis described above. Following 2−3 weeks of treatment with Gemcitabine, SGI-7079, or a combination of both (Fig. 7a), tumor weights (Fig. 7b, c) and metastases (Fig. 7d) were evaluated. In line with our in vitro data, inhibition of Axl signaling not only augmented the capacity of Gemcitabine to reduce tumor burden in vivo (Fig. 7c), but a notable and profound effect on tumor mass was noted in the majority of mice receiving the combination treatment (Fig. 7b, c), with two mice experiencing complete tumor regression. Interestingly, while SGI-7079 alone had no effect on tumor burden, mono and combination treatments with SGI-7079 reduced metastasis in 60% and 100% of the mice, respectively (Fig. 7d), confirming previous links between Axl and EMT [35].

Consistent with our human serum sample analyses (Fig. 4d–f), a significant and consistent increase in murine 14-3-3ζ serum levels was observed in mice receiving Gemcitabine, which was irrespective of Axl inhibition. Acknowledging that Axl is also expressed on immune cells and targeting Axl signaling in combination with Gemcitabine can affect the immune cell landscape of the tumor microenvironment [11], we evaluated the infiltration of YM-1-positive M2 macrophages (Fig. 7f and Supplementary Fig. S10A) and the percentage of CD45+ F4/80+ macrophages (Supplementary Fig. S10B) in the pancreata of treated mice by IHC and flow cytometry, respectively, and observed a marked but nonsignificant reduction in these cell populations. Lastly, to apply these findings to the Bailey et al. dataset series, we stratified patients based on *14-3-3ζ* and *AXL* expression and observed that the overall survival of patients expressing both genes at high levels (top quartile) was significantly lower ($p = 0.0126$) (Fig. 6g and Supplementary Fig. S10C), demonstrating a significant biological relationship between 14-3-3ζ and Axl in PDAC.

## Discussion

It is well accepted that TAMs secrete factors that are anti-inflammatory or immunosuppressive [5]. Likewise, we now appreciate that they also promote wound healing, tumor growth and metastasis [36]; activate the CSC compartment [7]; and mediate radio [37] and chemoresistance [38]. However, no study to date has addressed the effect that post chemotherapy-induced apoptotic cell death can have on TAMs and how such an interaction may influence PDAC chemoresistance. Appreciating the observations that (1) CD163+ positive macrophages are present in high percentages following chemotherapy (Fig. 1a), (2) chemotherapy induces apoptosis in human PDAC tumors (Fig. 1a), and (3) a main function of macrophages is to eliminate apoptotic cells via phagocytosis (Fig. 1b) [17], we set out to dissect the effect that apoptotic cancer cells have on macrophages. The concept that macrophages respond to apoptotic cells is not new. As early as 1998, Peter Henson and colleagues showed that macrophages that have ingested apoptotic cells in vitro inhibit proinflammatory cytokine production, challenging the idea that phagocytosis of apoptotic cells by macrophages is a "quiet process" [39]. Specifically, they showed that phagocytosis of apoptotic cells inhibited macrophage production of proinflammatory cytokines, but increased production of TGF-ß1, PGE2, and PAF, three known active anti-inflammatory/suppressive factors [39]. In essence, their study revealed that macrophages are critical immune sensor cells that respond to specific scenarios, such as apoptosis induction, to inhibit the

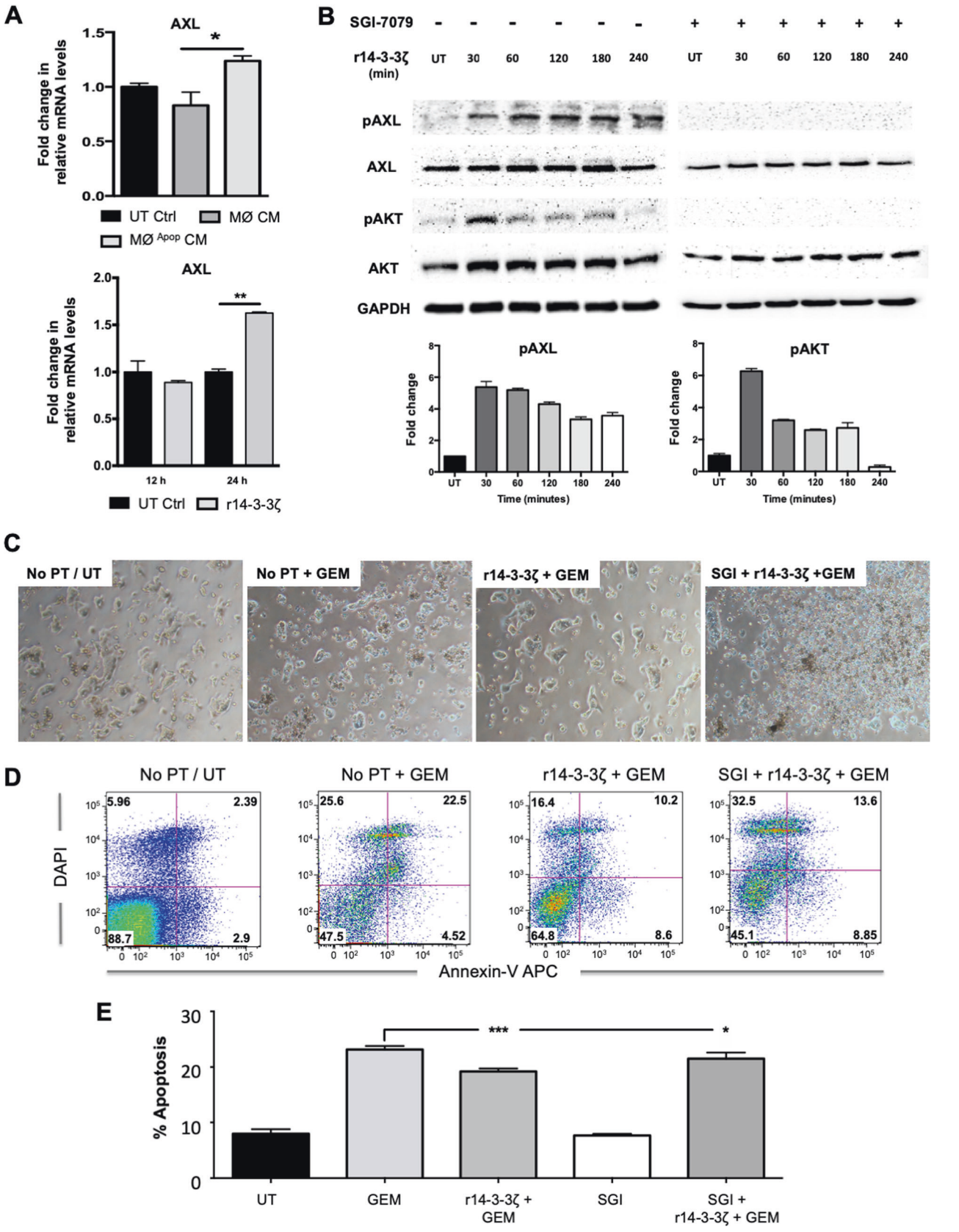
A
AXL
Fold change in relative mRNA levels
UT Ctrl
MØ CM
MØ Apop CM
AXL
12 h
24 h
UT Ctrl
r14-3-3ζ
B
SGI-7079
r14-3-3ζ (min)
UT 30 60 120 180 240
pAXL
AXL
pAKT
AKT
GAPDH
pAXL
pAKT
Fold change
Time (minutes)
C
No PT / UT
No PT + GEM
r14-3-3ζ + GEM
SGI + r14-3-3ζ +GEM
D
No PT / UT
No PT + GEM
r14-3-3ζ + GEM
SGI + r14-3-3ζ + GEM
DAPI
Annexin-V APC
5.96
2.39
88.7
2.9
25.6
22.5
47.5
4.52
16.4
10.2
64.8
8.6
32.5
13.6
45.1
8.85
E
% Apoptosis
UT
GEM
r14-3-3ζ + GEM
SGI
SGI + r14-3-3ζ + GEM

◀ **Fig. 6** 14-3-3ζ drives chemoresistance by activating AXL-mediated prosurvival pathways. **a** RTqPCR analysis of relative mRNA expression levels of Axl in Panc354 cells following no treatment (UT Ctrl), treatment with MØCM or MØ$^{Apop}$CM for 24 h (top), or treatment with 4 µg/ml of r14-3-3ζ for 12 or 24 h (bottom). mRNA expression levels are normalized to ß-actin levels, and data are represented as fold change compared to UT Control (set at 1.0). $n = 4$ samples per group. Statistical significance: $*p < 0.05$, $**p < 0.01$. **b** Expression of p-Axl, total Axl, p-AKT or total AKT, detected by western blotting, in total lysates from synchronized Panc354 cells treated for the indicated minutes with r14-3-3ζ in the presence or absence or SGI-7079 (1 µM). GAPDH was used as a loading control (top). Fold change in phosphoprotein levels determined by densitometric analysis of two replicate experiments (bottom). **c** Representative light micrographs, **d** representative flow cytometric analysis of Annexin-V staining and **e** quantification of total apoptosis in Panc354 cells 48 h post treatment with GEM. Cells were either (1) non-pretreated (No PT), (2) pretreated with r14-3-3ζ for 6 h, (3) pretreated with SGI-7079 (SGI; 1 µM) for 5 h, or (4) pretreated with SGI (1 µM) for 5 h followed by r14-3-3ζ for 6 h prior to challenge with or without (UT) 1 µg/ml of GEM. Average of three independent experiments ($n = 3$ samples/experiment). Statistical significance: $*p < 0.05$, $***p < 0.001$

release of toxic and immunogenic byproducts of apoptosis, but at the same time stimulating an anti-immune phenotype to control inflammation. Herein, we build upon the study by Fadok et al. and others that have followed [40], focusing our attention on how macrophages respond to chemotherapy-induced apoptotic cells in the context of cancer.

We provide data to show that CD163 macrophages are present together with apoptotic cells in PDAC tumors following chemotherapy, macrophages can readily phagocytose apoptotic PDAC cells, their phagocytosis promotes macrophage M2-like polarization and the subsequent release of factors that can act on naïve PDAC cells rendering them resistant to chemotherapeutic challenge. Interestingly, it appears as though *TP53* mutant cells benefit more from these secreted factors, which may be due to a synergistic effect between the pathways activated by the MØCM and the impaired p53-triggered apoptosis in these cells. More research is still required to dissect this observation. Using an unbiased MS approach to identify secreted factors unique to macrophages that have ingested apoptotic cells in vitro, we identified 14-3-3ζ as a potential driver of TAM-mediated chemoresistance. It is important to note that it has been shown by Miller and colleagues that Gemcitabine and other chemotherapeutics can also induce necroptosis, a more recently described mechanism of cell death that denotes coordinated cellular necrosis, and one that has been described as an unexpected driver of pancreatic oncogenesis [41]. As such, we cannot rule out that PDAC death by other mechanisms may have also influenced our secretome analysis.

14-3-3ζ, the top candidate protein investigated in this study, is one of seven isoforms of the larger 14-3-3 protein family, which participate in many biologic processes including DNA replication, DNA repair, apoptosis and malignant transformation [20]. 14-3-3ζ, in particular, can act as direct suppressor of apoptosis by binding to and sequestering the proapoptotic mediators BCL2-associated agonist of cell death (Bad) and BCL2-associated X protein (Bax) [28] (Fig. 8). In addition, 14-3-3ζ has been shown to play a central role in tumorigenesis and progression in many cancer types, and it has been proposed as a novel molecular target for cancer therapy [42]. Endogenous 14-3-3ζ forms both homodimers and heterodimers with other 14-3-3 family members, inhibiting inherent cellular antitumor pathways such as apoptosis and promoting cell cycle, proliferation and adhesion [28] (Fig. 8). We hypothesize that during chemotherapy, endogenous 14-3-3ζ is in association with intracellular proteins and that additional exogenous 14-3-3ζ provided by macrophages is necessary to enable PDAC cells, via phospho-Axl signaling mediators such as Akt, to overcome prolonged and continuous chemotherapeutic insult (Fig. 8). This hypothesis is supported by our two in vivo studies where we show that (1) murine PDAC tumors respond significantly better to Gemcitabine when macrophages are deleted, and (2) Axl signaling inhibition in vivo with SGI-7079 significantly augmented the effects of Gemcitabine. Along these lines it is important to discuss the recent work by Brekken and colleagues, where they show that targeting Axl in PDAC with the Axl inhibitor BGB324 also enhanced the therapeutic effects of Gemcitabine in vivo [11]. The authors demonstrate that Axl inhibition (1) promoted PDAC cell differentiation, (2) created an antitumor immune stimulatory microenvironment and (3) reduced the infiltration of protumor immune cells including TAMs. While our phenotypes with the Axl inhibitor SGI-7079 were very similar, the mechanism of action we propose is distinct but not mutually exclusive. Indeed, the effects observed by Brekken and colleagues using BGB324 may also be partially due to inhibiting 14-3-3ζ/Axl axis signaling, as much as our results may also be partially due to modulation of the tumor immune microenvironment and/or a reduction in TAM infiltration, although the reduction we observed was not significant in our syngeneic model using SGI-7079 (Supplementary Fig. S10B). Nonetheless, the fact that targeting Axl may result in the modulation and inhibition of multiple overlapping pathways that are essential for PDAC-resistant mechanisms is in and of itself interesting and positions Axl as a target of significant interest.

At the same time, the elimination of macrophages achieved similar effects as those achieved with SGI-7079, suggesting that targeting TAMs also holds significant clinical potential. It is important to note that while clodronate has been shown to primarily affect phagocytic cells (i.e. macrophages), we cannot rule out that 5 weeks of clodronate treatment may have also affected other cellular

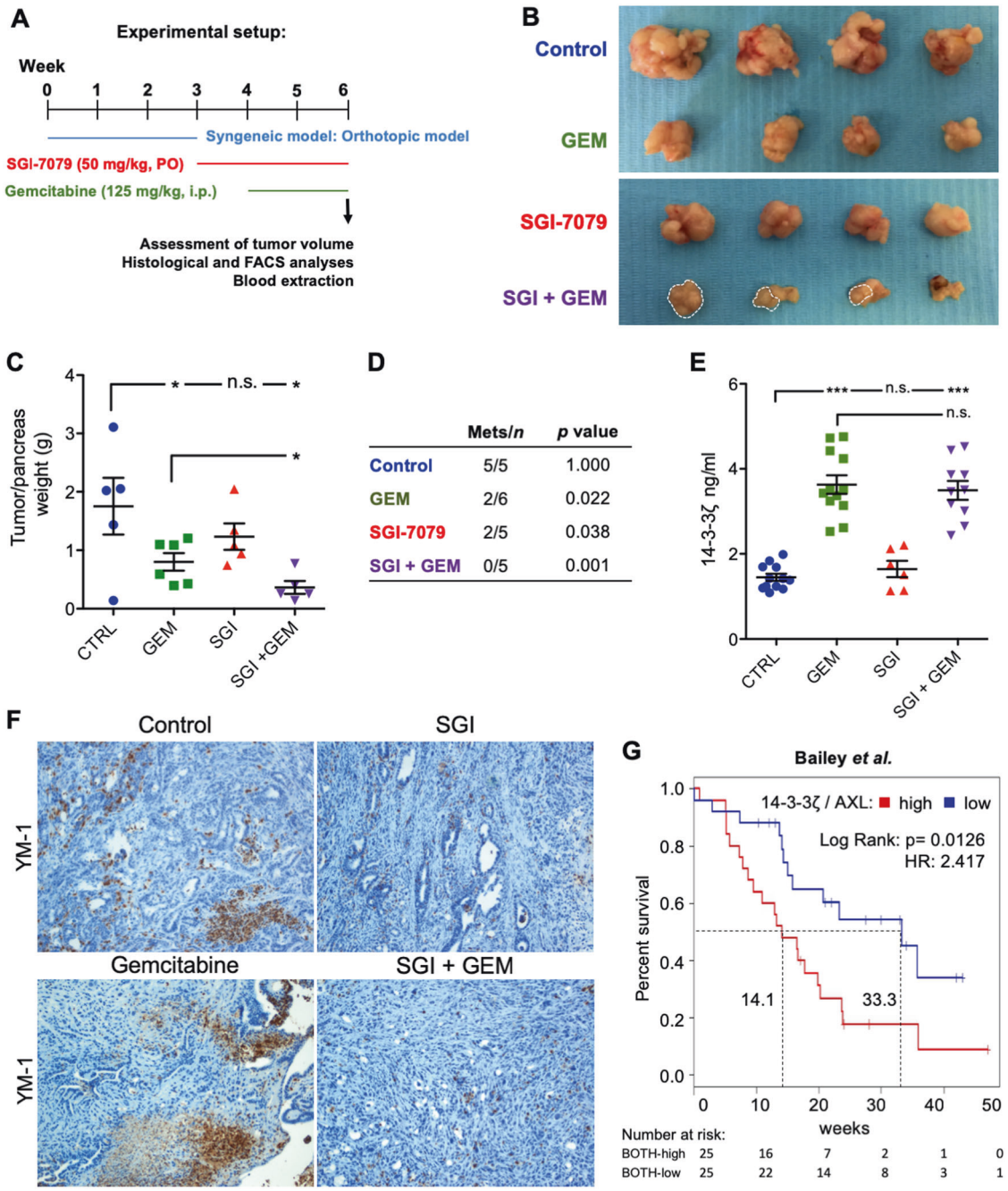


**Fig. 7** Inhibition of Axl with SGI-7079 potentiates the anticancer efficacy of Gemcitabine. **a** Experimental set-up for SGI-7079 (SGI) and Gemcitabine (GEM) in vivo efficacy studies in a syngeneic orthotopic tumor model. GEM (125 mg/kg twice/weekly) and SGI (50 mg/kg PO QD). **b** Representative images (dashed line marks tumor area), **c** average weight of pancreata ($n = 5$ mice per treatment group) and **d** summary of in vivo metastasis (including lung, liver, spleen, diaphragm, lymph nodes or peritoneum). Shown are the number of mice with metastases/total number of mice examined ($n$), and the respective $p$ value determined by Chi-square test (95% CI). **e** Quantification of 14-3-3ζ levels in the serum of mice 24 h post indicated treatment. **f** IHC analysis of YM-1 staining in FFPE samples of pancreata from indicated treatment groups. **g** Kaplan–Meier curve showing the overall survival of PDAC patients, stratified according to the median value of *14-3-3ζ* and *AXL* expression (both high vs. both low) ($n = 50$). The hazard ratio (HR) and number of patients at risk are shown. Statistical significance: $*p < 0.05$, $***p < 0.001$, n.s. = not significant. CTRL = control. PDAC pancreatic ductal adenocarcinoma

subtypes present in the microenvironment, increasing its antitumor properties. Nonetheless, we conclude that the effect observed with clodronate and gemcitabine combination treatment was due to both macrophage elimination and gemcitabine-induced apoptosis induction. The latter has been extrapolated to the clinic in a dose-finding study by Nywening et al., where researchers showed that the addition of a small molecule CCR2 inhibitor PF-04136309 (an

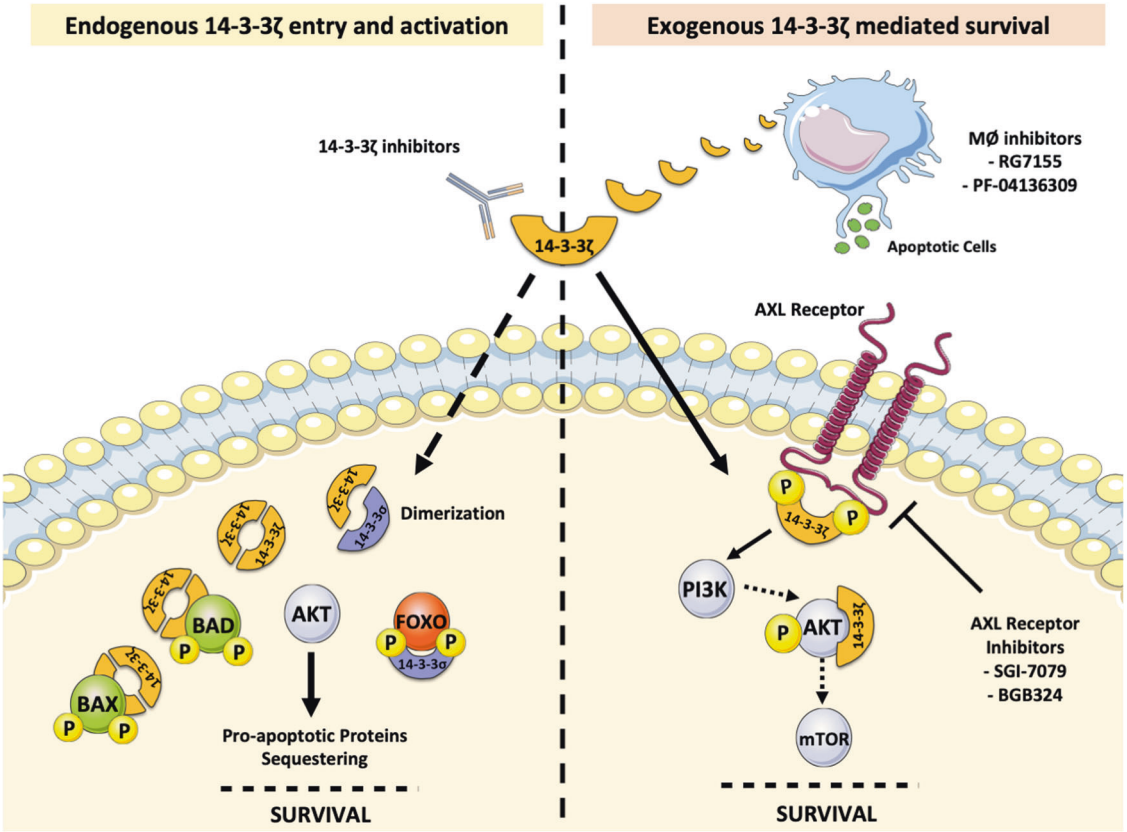


**Fig. 8** Model of the effects of endogenous and exogenous 14-3-3ζ on PDAC cell survival and chemoresistance. (Left) Endogenous 14-3-3ζ forms both homodimers and heterodimers with other 14-3-3 family members (e.g. 14-3-3σ), inhibiting inherent cellular antitumor pathways such as apoptosis by sequestering proapoptotic mediators such as BAD, BAX and FOXO. These interactions will inevitably promote cell cycle, proliferation and adhesion. (Right) During chemotherapy, endogenous 14-3-3ζ is in association with intracellular proteins. Exogenous 14-3-3ζ provided by macrophages that have phagocytosed chemotherapy-induced apoptotic PDAC cells can passively diffuse through the plasma membrane and interact with AXL tyrosine kinase receptor, resulting in its phosphorylation and subsequent activation/phosphorylation of downstream mediators such as AKT, which will promote survival in the presence of prolonged and continuous chemotherapeutic insult. From a clinical perspective, the prosurvival capacity of 14-3-3ζ can be inhibited by either inhibiting Axl phosphorylation with inhibitors such as SGI-7079 or BGB324, neutralizing 14-3-3ζ with antibody-based approached or eliminating macrophages and/or inhibiting their recruitment with compounds such as PF-04136309 (a CCR2 inhibitor) or the monoclonal antibody (RG7155) that blocks the dimerization interface of the CSF1 receptor (CSF1R). PDAC pancreatic ductal adenocarcinoma

inhibitor of monocyte recruitment) to FOLFIRINOX resulted in significant tumor shrinkage in 48% of patients [43], double the historical response rate of FOLFIRINOX alone. Whether a more potent effect would have been observed in combination with Axl inhibitors is still unknown but should be considered in light of our and Brekken and colleagues' findings. Lastly, it is likely that other antiapoptotic factors identified in the secretome from macrophages that had phagocytosed apoptotic cancer cells may also play a role in PDAC chemoresistance, and as such, inhibitors targeting these other factors may also be clinically beneficial. Apart from Hornerin, we also identified TIMP1 in $MØ^{Apop}CM$. Importantly, D'Costa et al. recently showed in the KPC mouse model of PDAC that Gemcitabine treatment increases TIMP1 expression, its expression correlates with resistance, TIMP1 inhibition resensitizes tumors to Gemcitabine and radiotherapy and a linear relationship between TIMP1 expression and infiltration by CD11b+ Gr1+ myeloid cells was observed [44].

In conclusion, we provide here a mechanistic analysis of the role of 14-3-3ζ in PDAC chemoresistance. Notably, while we propose a temporal order of events to explain our model, we cannot exclude that these events may also occur in a different order. Nevertheless, all of our data support the underlying observation that 14-3-3ζ is secreted by macrophages that have phagocytosed apoptotic PDAC cells, and upon interacting with Axl can mediate chemoresistance by activating prosurvival pathways. Since a relationship between 14-3-3ζ and Axl is strong in hepatocellular carcinoma (HCC) [29] and Axl is an accurate biomarker of cirrhosis and HCC development [45], we propose that 14-3-3ζ and Axl may represent markers that could putatively guide pancreatic cancer patient treatment. Indeed, we report here for the first-time detectable levels of 14-3-3ζ in serum

of 34 PDAC patients and in mice following chemotherapy. Of note, those patients that showed a significant increase in 14-3-3ζ showed a significant reduction in PFS and OS compared to patients where no changes in 14-3-3ζ levels were observed. While testing of a larger number of samples with preset extraction criteria would be necessary before definitive conclusions could be drawn, these data confirm that chemotherapy induces 14-3-3ζ expression in vivo and suggests that free 14-3-3ζ levels may have prognostic value. Finally, the role of 14-3-3ζ may be more pleiotropic than originally believed, affecting pathways other than apoptosis. For example, in a very recent study by Wang et al., the authors show that 14-3-3ζ delivered by exosomes can impair the antitumor function of tumor-infiltrating T lymphocytes in HCC [46], highlighting that more research is still needed to fully understand the broad role(s) of 14-3-3ζ in cancer. Nevertheless, this study details a new role for 14-3-3ζ in PDAC chemoresistance and at the same time emphasizes a unique regulatory mechanism where macrophages, specialized immune sensor cells, can respond to chemotherapy-induced apoptosis, initiating previously unappreciated pro-tumor/antiapoptotic mechanisms, thus challenging the idea that apoptosis of tumor cells is always beneficial.

## Materials and methods

### Primary human pancreatic cancer cells, patient samples, and macrophages

PDAC patient-derived xenografts (PDAC PDX) were processed and cultured as previously described [47]. Blood samples were obtained from PDAC patients and healthy donors with informed consent and with approval from the Ethics Committees of each respective hospital. Monocyte-derived macrophage cultures were established from CD14-positive monocyte-enriched cultures.

### Flow cytometry

For cell surface marker expression, refer to primary and secondary antibodies listed in Table S4. For all assays, DAPI was used to mark dead cells and data were analyzed with FlowJo 9.3 software (Tree Star Inc., Ashland, OR).

### Conditioned media (CM) experiments

Monocyte-derived macrophages were cultured with or without apoptotic PDAC cells for a total of 3−5 h. Apoptotic cells were removed, cultures were extensively washed and macrophages were cultured for an additional 24 h to allow for the accumulation of secreted factors. CM was used for WB or chemoresistance assays.

### In vivo assays

Wild-type C57Bl/6 8-week-old female mice were purchased directly from the Instituto de Investigaciones Biomédicas "Alberto Sols" Animal Facility (Madrid, Spain). Protocols were approved by the Universidad Autonoma de Madrid Ethics Committee (CEI 60-1057-A068) and La Comunidad de Madrid (PROEX 335/14). For syngeneic orthotopic experiments, murine PDAC tumor pieces (derived from a backcrossed K-Ras$^{+/LSL\text{-}G12D}$;Trp53$^{LSL\text{-}R172H}$;PDX1-Cre (KPC) mouse [48]) of approximately 20 mm$^3$ were orthotopically implanted into the pancreas of recipient C57Bl/6 mice. Treatments were initiated ~3 weeks post transplantation and pancreas and liver were harvested 5−6 weeks later. Numbers of mice required for each experiment (tumor progression, tumor weight, and histological analyses) were calculated on the basis of previously published work without prior power analysis. Age-matched animals with similar tumor burden were randomized and treated in groups of 5−6 mice. The investigators were not blinded during group allocation or when assessing the results or analyzing data.

### RNA preparation and RTqPCR

Total RNA was isolated by the GTC method. mRNA relative copy numbers were determined by RTqPCR using standard curves and normalized to ß-actin levels. Primers are listed in Table S5.

### Gene expression datasets and GSEA analyses

The gene expression datasets used in this study are publicly available. The dataset from Janky et al. [24] was downloaded from GEO (GSE62165); the dataset from Jandaghi et al. [25] from ArrayExpress (E-MTAB-1791); the dataset from Bailey et al. was included in a supplementary figure of their published work [26]; and the META dataset, containing datasets GSE15471, GSE16515, GSE22780, and GSE32688, was generated as described in [23].

### Proteomics analysis: sample preparation, mass spec (MS) and bioinformatic analysis

MS and MS/MS data were acquired using a LTQ-Orbitrap XL (ThermoFisher Scientific, Waltham, Massachusetts, USA). The 15 most intense doubly and triply charged peptide-ions were automatically chosen by the Xcalibur software (ThermoFisher Scientific) and fragmented, and MS data were processed to generate peak lists for protein identifications. Database searches were carried out with MASCOT server. The SwissProt database was used, allowing two missed cleavages, carbamidomethyl (C) as

fixed modification, oxidation (M) and phosphorylation (ST) as variable modifications. The peptide tolerance was set to 30 ppm and the MS/MS tolerance to 0.8 Da. See Supplementary Tables S1 and S2.

## Statistical analyses

Results are presented as means ± standard error of the mean (sem) unless stated otherwise. All experiments were performed at least twice. Pair-wise multiple comparisons were performed with one-way ANOVA (two-sided) with Bonferroni adjustment. When indicated, and if the sample distribution was considered normal using the D'Agostino-Pearson omnibus test, a paired or unpaired $t$ test was performed. $p$ values $< 0.05$ were considered statistically significant. All analyses were performed using GraphPad Prism version 5.0c (San Diego California USA).

**Acknowledgements** We are indebted to José Germán Casas for CD14-enriched monocyte preparations, Carmen Sánchez Palomo and Esperanza Macarena Rodriguez Serrano for IHC and histological assistance, and María González Dionis for in vitro technical assistance. The research was supported by a Rámon y Cajal Merit Award (RYC-2012-12104) from the Ministerio de Economía y Competitividad, Spain (BS, Jr.), a Clinic and Laboratory Integration Program (CLIP) grant from the Cancer Research Institute (CRI), NY (BS, Jr.), a Coordinated grant (GC16173694BARB) from the Fundación Asociación Española Contra el Cáncer (AECC) (AC and BS, Jr.), Fondo de Investigaciones Sanitarias (FIS) grants PI15/01507 (BS, Jr.), PI15/01715 (LGB) and PI15/02101 (AC) (co-financed through Fondo Europeo de Desarrollo Regional (FEDER) "Una manera de hacer Europa") from the Instituto de Salud Carlos III (ISCIII), Spain, funding from the Biomedical Research Network in Cancer (CIBERONC:CB16/12/00446) for clinical sample and data collection (AC), funding from the Austrian Science Fund (FWF-B27361) and Ingrid Shaker-Nessmann Foundation for Cancer Research (PM), a Max Eder Fellowship of the German Cancer Aid (111746) (PCH), and by the German Research Foundation (DFG, CRC 1279 "Exploiting the human peptidome for Novel Antimicrobial and Anticancer Agents") (PCH).

## Compliance with ethical standards

**Conflict of interest** The authors declare that they have no conflict of interest.



## References

1. Rahib L, Smith BD, Aizenberg R, Rosenzweig AB, Fleshman JM, Matrisian LM. Projecting cancer incidence and deaths to 2030: the unexpected burden of thyroid, liver, and pancreas cancers in the United States. Cancer Res. 2014;74:2913–21.
2. Hidalgo M, Cascinu S, Kleeff J, Labianca R, Lohr JM, Neoptolemos J, et al. Addressing the challenges of pancreatic cancer: future directions for improving outcomes. Pancreatology. 2015;15:8–18.
3. Ko AH. Progress in the treatment of metastatic pancreatic cancer and the search for next opportunities. J Clin Oncol. 2015;33:1779–86.
4. Wang WQ, Liu L, Xu HX, Wu CT, Xiang JF, Xu J, et al. Infiltrating immune cells and gene mutations in pancreatic ductal adenocarcinoma. Br J Surg. 2016;103:1189–99.
5. Sica A, Allavena P, Mantovani A. Cancer related inflammation: the macrophage connection. Cancer Lett. 2008;267:204–15.
6. Nielsen SR, Quaranta V, Linford A, Emeagi P, Rainer C, Santos A, et al. Macrophage-secreted granulin supports pancreatic cancer metastasis by inducing liver fibrosis. Nat Cell Biol. 2016;18:549–60.
7. Sainz B Jr., Carron E, Vallespinos M, Machado HL. Cancer stem cells and macrophages: implications in tumor biology and therapeutic strategies. Mediators Inflamm. 2016;2016:9012369.
8. Sainz B Jr., Martin B, Tatari M, Heeschen C, Guerra S. ISG15 is a critical microenvironmental factor for pancreatic cancer stem cells. Cancer Res. 2014;74:7309–20.
9. Sainz B Jr., Alcala S, Garcia E, Sanchez-Ripoll Y, Azevedo MM, Cioffi M, et al. Microenvironmental hCAP-18/LL-37 promotes pancreatic ductal adenocarcinoma by activating its cancer stem cell compartment. Gut. 2015;64:1921–35.
10. Ireland L, Santos A, Ahmed MS, Rainer C, Nielsen SR, Quaranta V, et al. Chemoresistance in pancreatic cancer is driven by stroma-derived insulin-like growth factors. Cancer Res. 2016;76:6851–63.
11. Ludwig KF, Du W, Sorrelle NB, Wnuk-Lipinska K, Topalovski M, Toombs JE, et al. Small-molecule inhibition of Axl targets tumor immune suppression and enhances chemotherapy in pancreatic cancer. Cancer Res. 2018;78:246–55.
12. Weizman N, Krelin Y, Shabtay-Orbach A, Amit M, Binenbaum Y, Wong RJ, et al. Macrophages mediate gemcitabine resistance of pancreatic adenocarcinoma by upregulating cytidine deaminase. Oncogene. 2014;33:3812–9.
13. Zhang X, Chen Y, Hao L, Hou A, Chen X, Li Y, et al. Macrophages induce resistance to 5-fluorouracil chemotherapy in colorectal cancer through the release of putrescine. Cancer Lett. 2016;381:305–13.
14. Vakkila J, Lotze MT. Inflammation and necrosis promote tumour growth. Nat Rev Immunol. 2004;4:641–8.
15. Byers LA, Diao L, Wang J, Saintigny P, Girard L, Peyton M, et al. An epithelial-mesenchymal transition gene signature predicts resistance to EGFR and PI3K inhibitors and identifies Axl as a therapeutic target for overcoming EGFR inhibitor resistance. Clin Cancer Res. 2013;19:279–90.
16. Hu H, Hang JJ, Han T, Zhuo M, Jiao F, Wang LW. The M2 phenotype of tumor-associated macrophages in the stroma confers a poor prognosis in pancreatic cancer. Tumour Biol. 2016;37:8657–64.
17. Duvall E, Wyllie AH, Morris RG. Macrophage recognition of cells undergoing programmed cell death (apoptosis). Immunology. 1985;56:351–8.
18. Olive KP, Jacobetz MA, Davidson CJ, Gopinathan A, McIntyre D, Honess D, et al. Inhibition of Hedgehog signaling enhances delivery of chemotherapy in a mouse model of pancreatic cancer. Science. 2009;324:1457–61.
19. Kobayashi R, Deavers M, Patenia R, Rice-Stitt T, Halbe J, Gallardo S, et al. 14-3-3 zeta protein secreted by tumor associated monocytes/macrophages from ascites of epithelial ovarian cancer patients. Cancer Immunol Immunother. 2009;58:247–58.
20. Masters SC, Fu H. 14-3-3 proteins mediate an essential anti-apoptotic signal. J Biol Chem. 2001;276:45193–200.
21. Khorrami A, Bagheri MS, Tavallaei M, Gharechahi J. The functional significance of 14-3-3 proteins in cancer: focus on lung cancer. Horm Mol Biol Clin Investig. 2017;32:1868–91.

22. Klemm C, Dommisch H, Goke F, Kreppel M, Jepsen S, Rolf F, et al. Expression profiles for 14-3-3 zeta and CCL20 in pancreatic cancer and chronic pancreatitis. Pathol Res Pract. 2014;210:335–41.
23. Martinelli P, Carrillo-de Santa Pau E, Cox T, Sainz B, Jr. Dusetti N, Greenhalf W, et al. GATA6 regulates EMT and tumour dissemination, and is a marker of response to adjuvant chemotherapy in pancreatic cancer. Gut. 2016;66:1665–76.
24. Janky R, Binda MM, Allemeersch J, Van den Broeck A, Govaere O, Swinnen JV, et al. Prognostic relevance of molecular subtypes and master regulators in pancreatic ductal adenocarcinoma. BMC Cancer. 2016;16:632.
25. Jandaghi P, Najafabadi HS, Bauer AS, Papadakis AI, Fassan M, Hall A, et al. Expression of DRD2 is increased in human pancreatic ductal adenocarcinoma and inhibitors slow tumor growth in mice. Gastroenterology. 2016;151:1218–31.
26. Bailey P, Chang DK, Nones K, Johns AL, Patch AM, Gingras MC, et al. Genomic analyses identify molecular subtypes of pancreatic cancer. Nature. 2016;531:47–52.
27. Eng EW, Bettio A, Ibrahim J, Harrison RE. MTOC reorientation occurs during FcgammaR-mediated phagocytosis in macrophages. Mol Biol Cell. 2007;18:2389–99.
28. Matta A, Masui O, Siu KW, Ralhan R. Identification of 14-3-3zeta associated protein networks in oral cancer. Proteomics. 2016;16:1079–89.
29. Reichl P, Dengler M, van Zijl F, Huber H, Fuhrlinger G, Reichel C, et al. Axl activates autocrine transforming growth factor-beta signaling in hepatocellular carcinoma. Hepatology. 2015;61:930–41.
30. Kariolis MS, Miao YR, Diep A, Nash SE, Olcina MM, Jiang D, et al. Inhibition of the GAS6/AXL pathway augments the efficacy of chemotherapies. J Clin Invest. 2017;127:183–98.
31. Korshunov VA. Axl-dependent signalling: a clinical update. Clin Sci (Lond). 2012;122:361–8.
32. Powell DW, Rane MJ, Chen Q, Singh S, McLeish KR. Identification of 14-3-3zeta as a protein kinase B/Akt substrate. J Biol Chem. 2002;277:21639–42.
33. Wu G, Ma Z, Hu W, Wang D, Gong B, Fan C, et al. Molecular insights of Gas6/TAM in cancer development and therapy. Cell Death Dis. 2017;8:e2700.
34. Kirane A, Ludwig KF, Sorrelle N, Haaland G, Sandal T, Ranaweera R, et al. Warfarin blocks Gas6-mediated Axl activation required for pancreatic cancer epithelial plasticity and metastasis. Cancer Res. 2015;75:3699–705.
35. Gjerdrum C, Tiron C, Hoiby T, Stefansson I, Haugen H, Sandal T, et al. Axl is an essential epithelial-to-mesenchymal transition-induced regulator of breast cancer metastasis and patient survival. Proc Natl Acad Sci USA. 2010;107:1124–9.
36. Kitamura T, Qian BZ, Pollard JW. Immune cell promotion of metastasis. Nat Rev Immunol. 2015;15:73–86.
37. Seifert L, Werba G, Tiwari S, Giao Ly NN, Nguy S, Alothman S, et al. Radiation therapy induces macrophages to suppress T-cell responses against pancreatic tumors in mice. Gastroenterology. 2016;150:1659–72 e1655.
38. Olson OC, Kim H, Quail DF, Foley EA, Joyce JA. Tumor-associated macrophages suppress the cytotoxic activity of antimitotic agents. Cell Rep. 2017;19:101–13.
39. Fadok VA, Bratton DL, Konowal A, Freed PW, Westcott JY, Henson PM. Macrophages that have ingested apoptotic cells in vitro inhibit proinflammatory cytokine production through autocrine/paracrine mechanisms involving TGF-beta, PGE2, and PAF. J Clin Invest. 1998;101:890–8.
40. Zhou N, Zhang Y, Zhang X, Lei Z, Hu R, Li H, et al. Exposure of tumor-associated macrophages to apoptotic MCF-7 cells promotes breast cancer growth and metastasis. Int J Mol Sci. 2015;16:11966–82.
41. Werba G, Seifert L, Miller G. Necroptotic cell death—an unexpected driver of pancreatic oncogenesis. Cell Cycle. 2016;15:2095–6.
42. Matta A, Siu KW, Ralhan R. 14-3-3 zeta as novel molecular target for cancer therapy. Expert Opin Ther Targets. 2012;16:515–23.
43. Nywening TM, Wang-Gillam A, Sanford DE, Belt BA, Panni RZ, Cusworth BM, et al. Targeting tumour-associated macrophages with CCR2 inhibition in combination with FOLFIRINOX in patients with borderline resectable and locally advanced pancreatic cancer: a single-centre, open-label, dose-finding, non-randomised, phase 1b trial. Lancet Oncol. 2016;17:651–62.
44. D'Costa Z, Jones K, Azad A, van Stiphout R, Lim SY, Gomes AL, et al. Gemcitabine-induced TIMP1 attenuates therapy response and promotes tumor growth and liver metastasis in pancreatic cancer. Cancer Res. 2017;77:5952–62.
45. Dengler M, Staufer K, Huber H, Stauber R, Bantel H, Weiss KH, et al. Soluble Axl is an accurate biomarker of cirrhosis and hepatocellular carcinoma development: results from a large scale multicenter analysis. Oncotarget. 2017;8:46234–48.
46. Wang X, Shen H, Zhangyuan G, Huang R, Zhang W, He Q, et al. 14-3-3zeta delivered by hepatocellular carcinoma-derived exosomes impaired anti-tumor function of tumor-infiltrating T lymphocytes. Cell Death Dis. 2018;9:159.
47. Mueller MT, Hermann PC, Witthauer J, Rubio-Viqueira B, Leicht SF, Huber S, et al. Combined targeted treatment to eliminate tumorigenic cancer stem cells in human pancreatic cancer. Gastroenterology. 2009;137:1102–13.
48. Hingorani SR, Wang L, Multani AS, Combs C, Deramaudt TB, Hruban RH, et al. Trp53R172H and KrasG12D cooperate to promote chromosomal instability and widely metastatic pancreatic ductal adenocarcinoma in mice. Cancer Cell. 2005;7:469–83.